IJAIPS International Journal of Advance Innovations in Pharmacy and Sciences

INTERNATIONAL JOURNAL OF ADVANCE INNOVATIONS IN PHARMACY AND SCIENCES

Volume 1
Issue 1
March-April 2025
www.ijaips.com

*Research Article*

# Formulation and Development of Mycophenolic Acid loaded Nanogel for the Effective Treatment of Psoriasis

**Arvind Kumar, Surendra Pratap Singh*, Jitendra Kumar Mallik**
Faculty of Pharmacy, P K University Shivpuri (M.P.) 473665

**ABSTRACT**
Formulation Development, of MPA-NLC and its therapeutic evaluation in imiquimod-induced model of psoriasis in albino mice. MPA loaded NLCs (MPA-NLCs) have been prepared using psoriasis in hot melt technique followed by homogenization and sonication. The different Excipients used for the preparation of MPA-NLC were glyceryl behenate, oleic acid, and span 80. Pareto and Box Behnken designs were used in the experiment's strategy to optimize MPA-NLCs and determine how the amount of lipid, homogenization speed, and surfactant concentration affect particle size, zeta potential, and entrapment effectiveness. A total 17 batch (F1-F17) were determined by the design of experiment and on the basis of PS, ZP and EE% batch F16 was selected as optimized batch and used for further studies. It was found that MPA-NLC exhibit nano-range particle size, narrow PDI, negative ZP, high EE% and drug loading. The morphological determination of MPA-NLC was carried out to determine the physical characteristic of MPA-NLC using SEM, TEM and AFM. It was found that MPA-NLC were spherical in shape with smooth surface, less agglomeration and uniform size distribution. Further, FTIR, XRD and DSC studies were also performed to determine the compatibility and structural change in MPA- NLC. The FTIR study showed amorphous transition and entrapment of MPA in the lipid matrix due to the presence of broad peaks in the spectra. indings indicates that the developed MPA-NLC nanogel for topical administration could be a rational strategy to attain augmented therapeutic attributes of MPA, without or having limited serious adverse effects in psoratic individuals. However, further studies are required to validate the efficacy of developed MPA- NLC nanogel in clinical subjects bearing psoriasis and related issues.

**KEYWORDS**: MPA- NLC nanogel , SEM, TEM, AFM Box Behnken designs, QbD

## INTRODUCTION

Psoriasis is a chronic autoimmune disease affecting 5% of the population in the world. According to Hippocrates (460-377 BC), the word psoriasis is obtained from the word psora meaning “to itch”. Psoriasis can be defined as a non-communicable disease characterized by hyper- proliferative epidermis[1], inflamed with red patches, dry and scaly. The most often affected area are scalp region, joints especially knees and elbows, palms and soles etc[2]. The condition affects both the sexes equally and can be visible at any age, however it is most common in the earliest stages of life between the ages of 15 and 25. The visible scales on skin generate humiliation among the patient and causes psychological,[3]

***Corresponding Author:**
**Surendra Pratap Singh Parihar**
Faculty of Pharmacy, P K University Shivpuri (M.P.) 473665
Email: spspharma2001@gmail.com
**Article Received: 10 March 2025**
**Article Revised and accepted: 25 April 2025**
This article can be accessed online on www.ijaips.com

socio-economic and emotional disbalance among them. The symptoms of psoriasis vary from visibility of ulcers on skin to the degeneration of nail followed by arthritis among 10-30% of the patients. Other than arthritis, one of the most significant issues associated with psoriasis is Crohn's disease, an inflammatory bowel ailment [4]. Both genetic and the environmental (alcohol, cigarettes, illnesses, drugs, stress) factors are responsible for activating the cytokines responsible for psoriasis excavation [5].

socio-economic and emotional disbalance among them. The symptoms of psoriasis vary from visibility of ulcers on skin to the degeneration of nail followed by arthritis among 10-30% of the patients. Other than arthritis, one of the most significant issues associated with psoriasis is Crohn's disease, an inflammatory bowel ailment [4]. Both genetic and the environmental (alcohol, cigarettes, illnesses, drugs, stress) factors are responsible for activating the cytokines responsible for psoriasis excavation [5].

Psoriasis is diagnosed on the basis of clinical investigations, showing symptoms like skin rash, scally patch, altered nails, joint inflammation, etc. Patients may occasionally have unusual skin sores that need to be differentiated from unidentified skin symptoms such as scalp scaling, isolated flexural erythema, or genital lesions, as well as mycosis fungicides, seborrheic dermatitis[6], tinea, and discoid lupus.

For the purpose of diagnosing psoriasis, the silvery white scales with red or dark pink lesions having noticeable margins may be marked for identification[7]. When the damp skin is scraped off, microscopic blood clots can be seen below the scales, which are visible beneath the pink, sensitive, wet skin. Sometimes, scraping, skin biopsies, and blood tests are also required to confirm the diagnosis of psoriasis [8]. The severity of the disease ranges from flaky, inflamed surface to widespread pustular psoriasis. Based on the proportion of skin affected, doctors typically categorise psoriasis as moderate to severe to assist patients in receiving the best course of therapy.[9] In case of mild psoriasis: Approximately 3% of the body surface is affected. In most situations, psoriasis affects less than 2% of the skin. In case of severe psoriasis: around 10% of the body surface is affected[10].

Topical application is an appealing path for both local and systemic treatment. Medication administration through the skin is regarded as a viable means of treating local dermatologic disorders[11]. It can infiltrate deep down into the skin and thereby have greater retention. Because of their structure and composition, they are considered more potent and less toxic than conventional dosage forms. Attempts are being made in the design of topical delivery systems to use drug delivery systems that ensure ample confinement or penetrance of the medicine within or through the skin to improve drug localization and limit systemic effects, or to assure adequate percutaneous retention.[12] Topical formulations can reduce GI discomfort, prevent drug degradation in the liver, and increase medication bioavailability. They offer their activity directly at the activity spot. Agel is a cross- linked 3-dimensional matrix made up of specific gelling materials mixed with an ample but comparatively large amount of liquid to form a persistent inflexible network structure that immobilizes the liquid continuous phase within[13]. The underlying components that make up the gel system may be inorganic particles or natural macromolecules, which are essentially polymers and their physical or chemical interactions, can form crosslinks. This results in the differentiation of gel into physical and chemical gel structures[14].

Chemical gels are formed due to the formation of irreversible covalent bonds, while physical gels are caused by more unstable and reversible discretionary intermolecular forces, such as hydrogen bonds, electrostatic associations, dipole-dipole interaction, Vander Waals forces, and hydrophobic forces[15].The U.S.P. delineates gels as a semisolid structure composed of a dispersion of either large organic molecules or small inorganic particles encased and inter-penetrated by a liquid (Luengas-Martinez et al., 2022). Gels provide a two-phase composition under which inorganic particles are dispersed in the continuous phase rather than dissolved, while large organic fractions are solubilized in the continuous phase and randomly contrived in the adaptable chains[16].

## MARTIAL AND METHOD

### Material

API and all Excipients were used as Analytical Grade.

### Method

#### Analytical determination of MPA by HPLC

High-performance liquid chromatography (HPLC) is a method that utilizes a reverse-phase C18 column for analytical determination of MPA. The mobile phase was composed of methanol (A) and acetate buffer (B) adjusted at pH above 6 using acetic acid. During analysis, 20 µL of samples were injected into the system, and the separation process was conducted. Both the phases were taken in a ratio of 70:30v/v (A: B) with a flow rate of 1.5 ml/min for a period of 15 minutes. The study was conducted at temperature set at 55 °C, using a 251 nm detection wavelength. To ensure the reliability and accuracy of the results, the analysis was carried out in triplicate [17].

#### Drug-lipid solubility studies

The solid lipid (SL) used to study the solubility of MPA's includes Precirol ATO5 (glyceryl palmitostearate), Dynasan 114 (trimyristate), Dynasan 116 (tripalmitate), Dynasan 118 (tristearate), and Compritrol 888 ATO (glyceryl behenate). The selection of SL was based on their solubility for MPA. To evaluate their solubility, 1g of each SL were melted in each test tube kept in a water bath at a temperature above 10°C of individual melting points. The melted lipid was added with increased amount of MPA (2 mg) until saturation was reached. The samples were then incubated in a refrigerated incubator shaker (Innova, model 4230) for 24 hrs. The amount required to obtain the saturated state was noted[18].

The appropriate liquid lipid (LL) for testing the solubility of MPA, capmule, oleic acid, and castor oil was taken. Excessive amounts of MPA were then dispersed in screw-capped tubes containing 2 ml of LL using a vortex mixer for 10 min. A

mechanical shaker (Orbit 300 Digital Multipurpose Shaker) was used to mechanically agitate the tubes for 24 hrs at 25°C at a constant speed of 200 rpm. The samples were then centrifuged for 10 min at 11000 rpm in a centrifuge. The supernatant was then collected and mixed with methanol. The diluted samples were then analyzed in triplicate using HPLC[19].

**Physiochemical compatibility and selection of a mixture of solid and liquid lipid**

The affinity of the drug on the lipids were assessed by SL and LL miscibility. For this, a binary combination of SL and LL was prepared based on lipids having maximum solubility of MPA in the melted state. The SL and LL were melted in a separate glass tube at a temperature above their melting points in a constant ratio of 1:1, and then mixed together to produce a binary mixture. At room temperature, the binary mixture was allowed to solidify. After some time, the presence of any separated layers in the congealed lipid mixture was visually checked in the glass tubes. Congealed lipid mixture that had been cooled was formed as a smear on hydrophilic filter paper. The filter paper was visually examined for signs of oil residue. To determine the miscibility, there should be no sign of oil droplets [20].

The best ratio of SL and LL having the best solubilizing tendency for MPA was determined by mixing the min a ratio of 90:10, 80:20, 70:30, 60:40, 50-50, 40:60, 30:70. 20:80 and 10:90. The binary mixture was melted above its melting point in a magnetic stirrer (REMI 5 - MLH Magnetic Stirrers) at 200 rpm for 1 hr at 80°C. About 2 mg of the MPA was added and NLC was prepared. The best ratio for NLC preparation was selected based on the maximum EE % inside the NLC [21].

**Selection of surfactant**

MPA-NLC was formulated by the hot homogenization method using different surfactants (Tween 80, Span 80, poloxamer 407, Poloxomer 188). The appropriate surfactant was selected based on optimum particle size of the NLCs prepared[22].

**Preparation of MPA-NLCs**

The MPA-NLCs were prepared by utilizing hot melt technique followed by homogenization and sonication. In a nutshell, a pre-emulsion was produced by dispersing the melting lipid phase at 80°C, which contained GB-SL and OA-LL. Pre-emulsion was set by dissolving drug (100 mg) in 1 ml of solvent containing a mixture of methanol: water in ratio 7:3. Span 80 is a lipophilic emulsifier that was added in then on-aqueous phase as a surfactant. A double distilled water (DDW) was heated at 80°C to obtain an aqueous phase. It was added drop-by-drop to the lipid phase to form a pre-emulsion, which was then homogenised for 10minutes at 15000 rpm using an Ultra-Turrax T25 homogenizer from IKA-Werke GmBH in Germany. The produced dispersion was sonicated for 2 min in a bath sonicator (ElmasonicS40, Elma, Singen, Germany). This emulsion was then chilled by constant stirring. The produced MPA-NLCs were subsequently characterized after being freeze-dried for 72 hours with a condenser surface set to -50°C in a Modulyo 4K freeze-dryer[23].

**Design of experiment using Box Behnken Design (BBD)**

**Significant QTPP and recognizing CQAs for applying the QbD approach**

For effective development of QbD, explaining the quality target product profile is a very important step that provides the ultimate blue print of the quality attributes of the proposed therapeutic product (Gurumukhi and Bari, 2020). The intended targets, such as skin penetration and increased therapeutic action of the drugs encapsulated in a NLC, were thoroughly researched to achieve a successful topical drug administration. In order to achieve these aims, it is crucial to emphasise the formulation's quality, safety, and effectiveness while taking into account the dosing method, stability of the excipient, experimental conditions, and product characteristics. This will help to provide better and more useful findings [24]. Identifying critical quality attributes (CQAs) and critical process parameters (CPPs) relevant to the formulation and process based on QTTP is the initial step in this technique.

In this study, the major CQAs and CPPs were identified based on aliterature survey of the previously published skill and knowledge about the factors affecting the quality of topical preparation (Khurana et al., 2020). Particle size (PS), entrapment efficiency (EE), and zeta potential(ZP) are the CQAs used for the investigation. Type of surfactant, surfactant concentration, homogenization duration (HT), homogenization speed (HS), and quantity of polymer are the CPPs used[25].

**Screening of factors using Pareto charts**

The variables impacting the correlations between various material and process variables and selected CQAs, Pareto charts were made. It eliminates potential factors that could have an impact on the product's quality, safety, and effectiveness. The Pareto charts were constructed using Minitab 17 statistical software. The critical quality attributes (CQAs) and critical material attributes (CMAs) chosen were the type of surfactant, surfactant conc., homogenization time (HT), homogenization speed (HS), amount of polymer, etc. using DoE to earmark and search the optimum levels of selected CMAs and/or CPPs[26].

**DoE (Box Behnken design) based optimization of MPA-loaded NLC**

After choosing the appropriate CMAs and CPAs through a Pareto chart, to earmark and search the ideal variables, the response surface methodology (RSM) was used with Design Expert. RSM is an empirical method used to study the relationship between the observed outcomes and the standard experimental condition. Statistical experiment design, mathematical model fitting for the coefficient, and response prediction based on experimental data are some of the key elements in this procedure [27].

The process of statistical analysis was conducted utilizing the Design Expert Statistical Software (version 11). To ascertain the correlation between three distinct factors and their corresponding three levels, the Box Behnken Design (BBD) was adopted. The CQAs (independent parameters) selected from Pareto chart analysis were HS in rpm (A), surfactant conc. in % v/v (B) and amount of polymer in mg (C). The CPPs (dependent parameter) chosen were PS in nm (Y1), EE in % (Y2), and ZP in mV (Y3). Based on a literature review, different levels were chosen. The overview of the BBD design used to optimize the formulation is shown in Table 1. The independent factors had a significant impact on the response parameter. The design was selected based on a few experimental combinations of the variables which can predict the accurate response function. The experimental design encompassed a total of 17 trial runs aimed at estimating the model. Table 9 gives detail about various runs generated by design depicting the combination of various parameters. The experimental data was analyzed through a polynomial equation using multiple regression analysis, with the intention of comprehending the interaction effects of CPPs.

Furthermore, a P-test was utilized to further validate these effects. The modeling of data was developed with quadratic model for a set of data that included linear, squared, and interaction terms. The goal of developing a quadratic model is often to identify the optimal conditions for the response variable of interest. This can be achieved by solving the quadratic equation for the independent variables that maximize or minimize the response variable. An alternative approach is to utilize RSM to generate a graphical representation of the response surface and identify the most favorable conditions.

A second-order equation, in the form of a best-fitting quadratic polynomial, was established for each response by evaluating the statistical significance of the CMPs through an ANOVA [28]. The results of the statistical analysis for the individual and interaction variables were compared to the estimated coefficients for the response. The main objective was to find out how well the model fits the data and identify any significant interaction effects. To evaluate the model adequacies several statistical metrics are commonly used in terms of correlation coefficient ($R^2$), adjusted $R^2$, predicted $R^2$, and adequate precision. Additionally, RSA was accomplished by introducing interaction relationships using the 2D-contour plots and 3D-response surface plots. These plots identify any significant interaction effects that may not be apparent from the statistical analysis alone using the desirability technique; optimization was done both numerically and graphically. To get the final, optimum, checkpoint analysis was conducted. The goal of evaluating model adequacy was to determine the effectively of model fitting the data and to identify any significant interaction effects[29].

**Table 1: Independent and dependent factors applied for BBD design**

| Independent Variables (CPPs) | Levels | | | Dependent variables (CPQs) |
|---|---|---|---|---|
| | High | Medium | Low | |
| Homogenization speed (rpm), A | 15000 | 10000 | 5000 | Particle size(nm),Y1 |
| Amount of polymer(mg),B | 200 | 150 | 100 | Entrapment efficiency (EE%). Y2 |
| Surfactant concentration (%v/v), C | 3 | 2 | 1 | Zeta Potential(mV),Y3 |

**Particle size, polydispersity index, and zeta potential**

The mean particle size and polydispersity index (size distribution, PDI) of MPA-NLCs were determined using the dynamic light scattering theory (DLST).The study was carried out at 25°C in Zetasizer Nano ZS (Malvern Instruments Ltd., Malvern, UK) at an angle of 160°. To avoid numerous scattering effects caused by interstellar particle interaction, the sample was diluted ten times with double- distilled water (DDW). The measurement of the samples was taken in triplicate[30].

The existence of charges on a particle's surface is a physical characteristic known as zeta potential, which foretells the stability of the system. It was determined using Zeta sizer Nano ZS (Malvern Instruments Ltd., Malvern, UK) for MPA-NLCs, based on a light scattering experiment and utilizing the Helmholtz- Smoluchowski equation based on electrophoretic mobility at a 20 V/cm field strength and 50 s /$cm^4$ conductivity .

**Entrapment Efficiency and drug loading**

Evaluate the entrapment efficiency (EE%) and drug loading of MPA- NLC, an indirect method that involved determining the concentration of free drug was used. The goal of this study was likely to determine how much of the drug was encapsulated within the NLCs.

The centrifuge tube utilized was MPA-NLC (1 ml) was diluted with methanol (5 ml). The obtained dilution was centrifuged for 20 min at 15000 rpm to separate the supernatant, which was then collected with a pipette. The concentration of the free drug was measured by HPLC. The entrapment efficiency and drug loading were calculated[33].

**Morphological evaluation**

**Scanning Electron Microscopy (SEM)**

SEM was used to determine the form and physical characteristics of MPA- NLC utilizing anS-3400 from Hitachi Ltd. In Tokyo, Japan. The sample was diluted with the required amount of DDW. On a metal stub, a drop of the developed dispersion was applied using double-adhesive carbon layer tape. The charges on the metal coversheet were decreased by coating with a gold covering. The coated samples were scanned using a SEM at an accelerating voltage of 20 kV, and images were captured using the software.

**Transmission electron microscopy (TEM)**

TEM examination was done to evaluate the shape and appearance of MPA- NLCs. A Morada Olympus SIS numerical camera and a JEOL 1010 (Tokyo, Japan) was used for the experiment. In this study, DDW split (1:10) was used to dilute the sample before it was deposited onto a carbon-coated copper grid. The surface had been thoroughly air dried before the grid was scanned in TEM at 200 kV. The images were captured using a sophisticated camera [34]

**Atomic Force microscopy (AFM)**

The morphological study of MPA-NLC was carried out through atomic force microscopy (AFM) (Nanosurf AG, Liestal, Switzerland).In this study, the non- contact mode (Tapping Mode) of experimentation was selected in order to avoid the damage caused to NLC due to contact between NLC and the tip of AFM(Slattery et al., 2018). The silicon probe-equipped pyramidal cantilevers were tuned to a frequency of 286kHz. The NLC dispersion(1:10v/v) was produced using DDW and sonicated to remove the adhered NLC. The prepared diluted sample was deposited on a mica plate and dried at room temperature using nitrogen gas to elude the movement of the particles[35].

**Fourier transform infrared spectroscopy**

FTIR studies were employed to determine the compatibility between the drug and the excipients. The spectra of Glyceryl behenate-solid lipid (GB-SL), Oleic acid- Liquid lipid (OA-LL), span 80, MPA, physical mixture (PM), and MPA-NLC was conducted using (Single Beam Bench top Bruker Laboratory FTIR Spectrometer, 2000 nm) spectrometer. The spectra were plotted between % transmittance and wave number (4000-600 $cm^{-1}$)

**X-RayDiffraction(XRD)**

The XRD was employed to determine the change in the crystalline material's phase during the formation of NLC. XRD was performed on MPA, GB-SL, PM, and a freeze-dried sample of MPA-NLC. The samples were flatted into a pellet between the glass slides and tested on a diffracto meter with Cu Ka radiation (40 kV and 40 mA). The diffraction profile was scanned at a 2θ value of 5 ° to 80 °C.

**Differential scanning calorimetry (DSC)**

DSC thermograms were collected in a 2910 TA calorimeter (TA Instruments, DE, USA) and analyzed with Thermal Solutions v.1.25 (TA Instruments, DE, USA) software to determine the melting point offormed NLC. The DSC analysis was conducted for GB-SL, MPA, PM, and a freeze-dried sample of MPA-NLC. In a hermetic aluminium pan, approximately 5 mg of sample was heated between 60 and 200 °C at a rate of 10 °C/min. An empty sealed pan was the standard. A nitrogen purge was employed to generate an inert gas atmosphere at a flow rate of 20 mL/min

According to ICH guidelines (Q1AR2), the MPA-NLC stability tests were carried out for six months. The samples were maintained at three distinct conditions: standard (25 ± 2°C and 65 % RH), accelerated (40 ± 2°C and 75 % RH), and cold (4± 2°C). The MPA-NLC was analyzed at a definite interval of 0, 1, 3, and 6 months for a change in particle size, ZP, and PDI. This study implies information about the stability of the formulation. Stability parameters were measured in triplicates[36].

**Preparation of MPA-NLC nanogel**

The MPA-NLC nanogel was developed by incorporating MPA-NLC into a Carbopol 934. Briefly, the Carbopol 934 was soaked in DDW for 1 hr to prepare gel (1%w/v). The MPA-NLC was incorporated into Carbopol 934 dispersion by stirring in a magnetic stirrer at 400 rpm for 1 hr. Further, the gel was neutralized using triethanolamine to produce desired viscosity. Similar to this, the MPA-dispersed gel was developed by combining Carbopol 934 (1%, w/v) with MPA that had been dissolved in methanol in the proper quantity. For 1 hr, the dispersion was stirred continuously at 400 rpm to generate a homogenous gel[37].

**Drug content and pH**

The drug content was determined by dissolving 1 g of MPANLC-nano gel (1%w/v) in100 ml of methanol that helped in calculating the amount of drug incorporated in MPA-NLC nanogel. The dispersion was blended for 2 hr and then centrifuged (11000 rpm 10 min) to completely extract the MPA from nano-gel matrix. After being filtered via 0.22m filter paper, the solution was analyzed in HPLC at 251 nm. The % drug content can be calculated. The pH of MPA-NLC stored at 25 ± °C and 65 % RH in a stability chamber was checked at intervals of 0, 30, 60, 90, and 180 days using a calibrated digital pH metre. The samples were measured in a triplicate.

**Viscosity**

The viscosity of the MPA-nano gel, MPA-gel, and blank gel at 25 °C were measured using a Brookfield viscometer (model DV-E). A spindle 6 was employed and dropped perpendicularly into a beaker containing 100 g, taking careto ensure that the spindle avoids touching the bottom of the container. It was spun from0.5to 100rpmto measure the viscosity [38].

**Spreadability**

Using Texture Analyzer TA. XT Plus, the spreadability of MPA-NLC nanogel, MPA-gel, and the blank gel was evaluated (Stable Micro Systems Ltd., Surrey, UK). It comprises of a female cone-shaped product holder and a male cone probe. The samples were placed in a female cone and allowed to set in advanced. The male cone was forced into the female cone and the degree of spreadability was determined by how easily the cone fits into the female cone.

**Texture analysis**

The consistency of MPA- NLC nanogel, MPA-gel, and blank gel was studied using a Texture Analyzer TA.XT. Plus from Stable Micro Systems Ltd. in Surrey, UK. In this experiment, 50g of MPA-NLC nanogel was put in a beaker with a smooth top to ensure that there were no air bubbles. Ananalytical probe of 40 mm was employed to compress the gel at a depth of 15 mm and a rate of 2 mm/s on two consecutive occasions with a 20 s interval between the readings. With the graphical representation of force against time, it was possible to derive the texture analysis curve of the gel which helps in evaluating variables such as firmness, consistency, cohesion, adhesiveness, and hardness [39].

**In-vitro release studies and kinetics**

The main purpose of this study was to examine the release behaviour of MPA-NLC and MPA-NLC nanogel over a period of 48 hrs. The study involved Franz diffusion cell having dialysis membrane (MW 12,000 Da) attached to both donor and receptor compartments. The dialysis membrane was activated prior to the experiment, by immersing it in a phosphate buffer (PBS, pH 6.8) for an extended period to induce stimulation. The PBS-filled receptor compartment was kept at a temperature of 37±2°C and subjected to agitation at 200 rpm. To increase the solubility of MPA in PBS, methanol was added as a co-solvent in the donor compartment filled with MPA-NLC (10mg/ml) (Shoukat et al., 2022). At regular intervals (0, 5, 10, 15, 30, 45 min, and 1, 2, 4, 8, 24, and 48 hrs) sample was withdrawn from the receptor compartment and replaced with a fresh PBS medium, ensuring sink conditions were maintained. After the addition of methanol, the samples were subjected to centrifugation at 5000 rpm for 10 min. The supernatant was collected for HPLC analysis at 251 nm. The drug release kinetics of MPA-NLC and MPA-nanogel were analysed through a graph between cumulative drug release per unit area against Vs. time [40].

The main purpose of this study was to examine the release behaviour of MPA-NLC and MPA-NLC nanogel over a period of 48 hrs. The study involved Franz diffusion cell having dialysis membrane (MW 12,000 Da) attached to both donor and receptor compartments. The dialysis membrane was activated prior to the experiment, by immersing it in a phosphate buffer (PBS, pH 6.8) for an extended period to induce stimulation. The PBS-filled receptor compartment was kept at a temperature of 37±2°C and subjected to agitation at 200 rpm. To increase the solubility of MPA in PBS, methanol was added as a co-solvent in the donor compartment filled with MPA-NLC (10mg/ml).

At regular intervals (0, 5, 10, 15, 30, 45 min, and 1, 2, 4, 8, 24, and 48 hrs) sample was withdrawn from the receptor compartment and replaced with a fresh PBS medium, ensuring sink conditions were maintained. After the addition of methanol, the samples were subjected to centrifugation at 5000 rpm for 10 min. The supernatant was collected for HPLC analysis at 251 nm. The drug release kinetics of MPA-NLC and MPA-nanogel were analysed through a graph between cumulative drug release per unit area against Vs. time[41] .

The study for release kinetics of a drug describes the characteristics of the delivery system along with its release mechanism. For this many kinetics models have been introduced which helps to understand the mechanism of release from the formulation. To establish an excellent parameter, multiple kinetic models can be employed to fit the data from in vitro study Different mathematical models, namely zero-order, first-order Higuchi and Korsmeyer equations, were used to analyse the in vitro release data of MPA in PBS 6.8. By using a variety of kinetics equations, it is possible.

**Animal Studies**

**Animal and ethical approval**

During the course of the investigation, male Swiss albino mice weighing between 25-30g were utilized. The research adhered to the guidelines and regulations established by the Committee for Control and Supervision of Experiments on Animals (CPCSEA) to ensure the ethical and compassionate treatment of the animals. The experimental techniques used in the study were authorized by the Institutional Animal Ethical Committee (IAEC). The animal mice and kept in polyacrylic cages at the recommended parameters of 25±2°C and 60 ± 5% RH. Throughout the investigation, the mice were provided with unlimited access to food and water to guarantee their welfare. Adhering to the guidelines and regulations established by the CPCSEA and the IAEC ensures that animal welfare is given the utmost priority and that ethical and compassionate practices are employed in animal experimentation.

**Skin permeation studies**

The skin permeation rates of MPA-NLC nanogel and MPA-gel by utilizing the abdominal skin of mice. In order to prepare the skin for study, the mice were humanely euthanize with100µL of a 10:1 mixture of ketamine (100 mg/mL) and xylazine (100 mg/mL) and its abdominal surface hair was removed using razor blade. The abdominal skin was then surgically extracted[41]. The skin was carefully cleansed with DDW to remove any redundant lipids and connective tissues to avoid any confounding variables that may affect the permeation results. Subsequently, the skin was immersed in pH 6.8 PBS to preserve its stability and integrity.

A skin permeation study was performed using the Franz diffusion cell (Perme Gear Inc. 4G-01-00-15-12), which had an effective permeation area of 1.76 $cm^2$ and a receptor volume of 8 ml. The receptor area was filled with pH 6.8 PBS that was kept at a temperature of 37± 0.5 °C while being constantly stirred in a magnetic stirrer at a rate of 400 rpm. The mentioned temperature and stirring rate were selected to replicate the physiological conditions of the skin. The mice skin was positioned between the donor and receptor compartment of the Franz diffusion cell. The donor compartment was filled with 500 mg of MPA-NLC nanogel. The MPA-NLC nanogel was compared to MPA gel to assess its permeation properties[43]. At predetermined intervals (0,5,10,15, 30,45,min, and 1, 2, 4, 8, and 24 hrs), sample was withdrawn from the receptor compartment and replaced with an equivalent amount of fresh diffusion medium in order to maintain the sink condition. The samples were diluted using methanol and analyzed under HPLC at 251nminorder to determine the MPA content. With the use of this data, a graph was generated between the cumulative quantity of drug release per unit area vs time, and the slope of the curve was used to examine the MPA release pattern and flux. By comparing the flux values of MPA-NLC nanogel and MPA gel, the enhancement ratio was computed, and the permeability coefficient was obtained using the formulation flux. The above mention procedure was applied for both MPA-nano gel and MPA gel mice skin[39].

**Drug retention studies on skin**

The skin retention study was carried out using same skin that was utilised for the ex-vivo skin permeation experiment. The skin was kept in a pH 6.8 PBS and cleaned thoroughly, ensuring that any residual drug was removed completely. Using the tape-stripping process, the skin's epidermis and dermis were separated, and the effectiveness of this approach was validated through the weighing of the segregated tissues. The tissues were then cut into pieces and homogenized in methanol. After homogenization, the tissue matrix and supernatant solution were separated by centrifugation at 11,000 rpm for 15 min. The amount of MPA in skin tissues was determined using HPLC at 251 nm.

**Dermato kinetics studies**

The dermato kinetic (PK) study was conducted according to a protocol similar to that of the ex-vivo skin permeation study, as elaborated in section 6.20.2. The research entailed analysing treated and non-treated groups (n=6) of both MPA-NLC nanogel and MPA gel formulations at various time intervals in both epidermis and dermis. To establish the DK parameter, it was crucial to assess drug retention on the skin, as well as its degradation and elimination through enzymes. Unlike the skin permeation study, this experiment involved periodic detachment of the skin from the diffusion cell, followed by washing with saline, and storage at 60 °C for 2-3 minutes. After that, forceps was used to divide the layers into dermis and epidermis. The parted skin layers were chopped into small pieces and absorbed in methanol for 24 hrs to eliminate any traces of drug. The extracted drug was then filtered and analyzed using HPLC at 251 nm, and the concentration of MPA(µg/$cm^2$) was determined in both skin layers. Non-compartmental pharmacokinetic modeling helps to determine DK parameters such as $C_{max}$, $T_{max}$, $AUC^{0-t}$, $AUC^{0-inf}$, t1/2, and MRT, which provides valuable insights into the drug retention, degradation, and elimination of the drug in different skin layers over time(Sharma et al., 2020), applied on the shaved region of mice at a dose of 50, 1000 and 2000 mg/kg body weight, and animals were examined for 14 days to determine mortality, redness, toxic symptoms, and any behavioural changes[40].

**Skin irritation studies**

In this assess any potential irritation on skin while using MPA-NLC nanogel. The Control

and Supervision of Experiments on Animals, CPCSEA Committee authorised this investigation on BALB/c mice. A total of three mice were utilized in the comparative analysis. Group A was treated with MPA-NLC nanogel, while group B was given a 0.8 percent v/v formalin solution, which served as the positive control for skin irritants, and group C was left untreated. To determine the degree of skin irritation, a Draize test was conducted, and scores were kept for a number of criteria including redness, skin rashes, erythema, and edema. Using razor blade, the hair of dorsal surface of mice was shaved in order to prepare the skin for examination. The formulation was applied to a1cm by1cm area of the mice's skin and left for 24hrs. The severity of skin irritation was assessed after application of MPA-NLC nanogel once a day for up to 7 days and grading the level of irritation using a scale ranging from 0 to 4 for redness, skin rashes, and erythema. A score of 0 meant that there was no erythema, while a score of 1 meant there was a faint reddening that might be patchy or widespread. A score of 2 indicated uniform moderate redness, while a score of 3 indicated severe redness. Ascoreof4 indicated fiery redness with edema[41].

## RESULT AND DISCUSSION

The HPLC technique was used to quantify MPA. The findings of HPLC study has been given in Figure 12a which illustrates the chromatogram of the MPA solution. The MPA retention time was determined as 3.6 minutes and a linearity assessment was carried out by plotting the MPA peak area against a concentration range of 1-6 g/mL. The correlation coefficient obtained from the graph was 0.9961

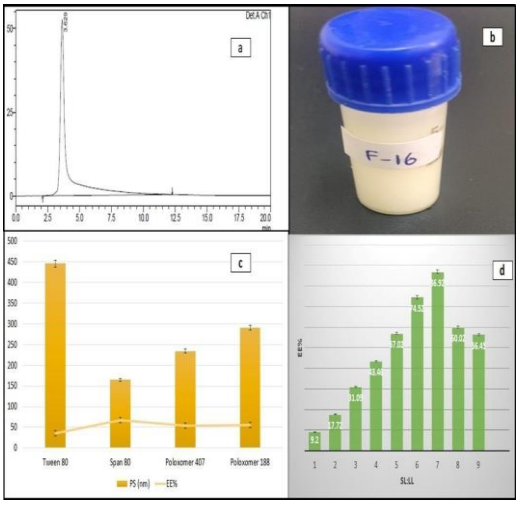


**Figure 1: a) A typical chromatogram of MPA. b) Formulation F-16. c) Graph depicting the best surfactant based on PS and EE% and (d) EE% of the SL: LL (1) 10:90, (2) 20:80, (3) 30:70, (4) 40:60, (5) 50:50, (6) 60:40, (7) 70:30, (8) 80:20, and (9) 90:10**

### Drug-lipid solubility studies

A semi-quantitative solubility investigation was conducted using several lipids, including Precirolato5 (glyceryl palmitostearate), Dynasan 114 (trimyristate), Dynasan116 (tripalmitate), Dynasan118 (tristearate), and Compritrol 888 ATO (glyceryl behenate). In the present study, Compritol 888 ATO (glyceryl behenate-GB) was chosen as the solid lipid for the formulation development since it had the maximum solubilization capability for MPA. The choice of liquid lipid was attained on the basis of quantitative solubility of MPA in different liquid lipids, including capmule, oleic acid, and castoroil. It was found that the solubility of MPA was maximum in oleic acid when compared to capmule, and castor oil.

### Study of physiochemical compatibility and selection of a mixture of solid and liquid lipid

The physical compatibility between the selected SL and LL was further assessed using filter paper analysis by visualizing the filter paper. Both the lipid remained uniformin a filter paper without any phase separation or remnant of liquid oil droplet on filter paper. The mixture was found to be homogeneous and there was no evidence of phase separation.

The ratio of SL:LL was selected based on the maximum entrapment of the MPA. It was observed that a ratio bearing 70:30 had the highest EE%, and any alteration in the ratio resulted in decrease in the drug entrapment content. This might be due to the saturation of MPA in the bilayer domain that destabilizes the membrane resulting in leakage of the content. Figure 12d provides the information pertaining to the selection of SL and LL ratio. The ratio of 70:30 resulted in efficient entrapment and the best physio-chemical characteristic and thus the respective ratio was selected for further studies.

### Selection of surfactant

To prepare NLC, the surfactant with the lowest PS and maximum EE % was chosen. The surfactant evaluated were tween 80, span 80, poloxamer 407, and poloxamer 188 for formulation development. It was found that span 80 showed the lowest PS and highest EE %. The resulting MPA-NLC was clear and transparent. Figure 12 c shows the PS and EE% of NLCs with different surfactant for the selection of surfactant.

### Preparation of MPA-NLCs

MPA-NLCs were developed by using hot melt homogenization method and freeze dried for further characterization study. The MPA-NLC

were applied with design of experiment for the optimization of best MPA-NLC formulation and was characterized further for PS, PDI, ZP, EE%, morphological evaluation using SEM, TEM, AFM, FTIR, XRD, DSC and stability studies.

**Design of experiment using BBD**

The design of experiments was applied for the optimization of MPA-NLCs to obtain a best PS, ZP and EE%, so that the formulation gives best result in regards with stability, and effectively.

**Significant QTPP and recognizing CQAs for applying the QbD approach**

The best possible QTTP were mentioned in table 7, which needs to be focused to ensure enhanced skin penetration, better skin moisture, drug retention on skin, better therapeutic benefits and better stability for the MPA-NLC and MPA- NLC nanogel. Similarly, identified CQAs to support QTTP were mentioned in table 8. A good CQAs in the optimized range helps to achieve the objective of QTTP in a better manner and ZPin mV (Y3).

**Table 2: QTTP element for the development of the MPA-NLC**

| QTTP elements | Target | Justification (s) |
|---|---|---|
| Dosage form | NLCs | Promotes skin moisture and enhances drug penetration via the skin. |
| Dosage type | Sustained release | It helps in superior skin penetration and retention |
| Dosage strength | 10mg | The recommended dose of the drug for psoriasis treatment administered through the skin. |
| Route of administration | Topical | Recommended route for the treatment of psoriasis |
| Appearance | White gel | Offers grace and a pleasing appearance |
| Skin permeation | Flux and skin retention that are higher | To obtain an optimal therapeutic result, it is necessary to attain higher drug penetration levels. |
| Stability | At varied storage temperatures for at least six months. | To ensure that drug retains its therapeutic benefits during the entire storage span. |
| Container and closure system | Collapsible opaque tube suitable for the product | To safeguard the formulation, extend its shelf life, and make administration easier |

**Table 3: Identified CQAs to support QTTP**

| CQA | Target | Justification (s) |
|---|---|---|
| PS | In a range of 100- 200 nm | Should be compact enough to allow for high drug retention and penetration in the dermal layer. |
| EE% | High | To reduce the high dosing of the drug |
| PDI | Below 1,around 0.2 | To maintain the homogeneity of the particles |
| ZP | Above30m Vor lessthan-30mV | To maintain the formulation's stability over a long length of time. |
| Skin retention | High | High skin retention is required to target the site effectively |
| Skin permeation | High | To obtain high efficacy of the drug |

**Screening of factors using Pareto charts**

The Pareto charts were prepared using Minitab 17 statistical software, to determine correlations between various material and process variables and selected CQAs. The various CPPs chosen were the type of surfactant, surfactant conc., homogenization time (HT), homogenization speed (HS), amount of polymer, etc. to earmark and search the optimum levels of selected CQAs and CPPs. Figure 13 depicts the Pareto charts used for screening these parameters. From the Paretocharts, the selected CPPs were HS in rpm (A), surfactant conc. in % v/v (B) and amount of polymerin mg (C)) and CQAs as PS in nm (Y1), EE in % (Y2),

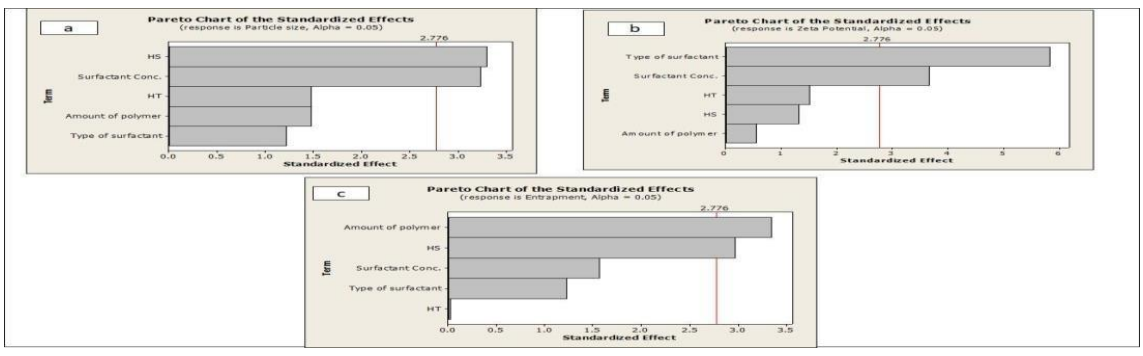


**Figure 2: Pareto charts used for screening the parameter. (a). Particle size,(b) zeta potential,(c) Entrapment efficiency**

**DoE (Box Behnken design) based optimization of MPA-loaded NLC**

The experimental data were obtained using Design-Expert software (version 11) which helped in developing the relation between various CPPs, and CQAs. Using BBD, 17 batches of MPA-NLCs were prepared by holt melt technique based on three level, three factor experimental study. The levels were distributed evenly, assigning the values -1, 0, and +1 as low, medium, and high. The CQAs selected were Y1, Y2, and Y3. The 17 experimental runs and their observed responses are listed in Table 9.

Based on the analysis, the best fit model related to various correlation coefficients $R^2$, predicted $R^2$, and adjusted $R^2$ were used to assists in determining how independent variables affects the responses. The adjusted $R^2$ in case of Y1 showed 0.1, Y2 showed 0.2 and Y3 showed 0.05 deviations when compared with predicted $R^2$. A value higher than 4 was the expected outcome for the ratio. The Y1/Y2/Y3ratio was31.069, 42.366,and19.205, respectively, indicating a sufficient signal that the design space can be explored through the utilization of this model. Regression analysis results for Y1, Y2, and Y3 have been presented in Table 10. A RSM study was carried out to analyse the best fit of the polynomial equations into linear, quadratic, and two-factor interaction (2F) models.

**Table 4: Summary of the result of regression analysis of responses Y1, Y2, and Y3**

| Response | Model | Std. Dev | $R^2$ | Adjusted $R^2$ | Predicted $R^2$ | Press |
|---|---|---|---|---|---|---|
| Y1 | Quadratic | 0.9935 | 0.9850 | 0.9850 | 0.8910 | 323.66 |
| Y2 | | 2.09 | 0.9733 | 0.9391 | 0.7377 | 299.74 |
| Y3 | | 1.12 | 0.9949 | 0.9884 | 0.9381 | 107.89 |

The mean particles size (Y1) of 17 batches was measured to be 192.27 nm, and varied in the range of161.80 to 200.31nm.The EE%(Y2) of the optimized batch was measured to be 88.92 % and varied in the range 88.92 to 59.02%. The ZP (Y3)of the optimized batch was measured at -53.5mV, varied in a range from-15.7 to -53.5 mV. The significance of each coefficient in equation (8), (9) and (10) was determined based on the p values listed in table 11.It suggests that small is the value of p, more significant is the corresponding coefficient. The p-value was analysed for Y1, Y2 and Y3. The ANOVA study for the quadratic model for Y1 suggests that it was significantly affected by A, B, and C among which A has a significant effect.

**Table 5: Analysis of factors and the irimpacton response: BBD Approach**

| S.No. | Run | Factor1 A: HS (rpm) | Factor 2 B:Amtof lipid(mg) | Factor3 C: Surfactant conc.(%) | Response 1:PSnm | Response 2: EE% | Response 3:ZP mV |
|---|---|---|---|---|---|---|---|
| 1 | F1 | 1 | -1 | 0 | 175.23 | 78.52 | -39.98 |
| 2 | F2 | 0 | 0 | 0 | 189.78 | 80.39 | -34.9 |
| 3 | F3 | -1 | 0 | -1 | 211.05 | 72.87 | -20.7 |
| 4 | F4 | 1 | 0 | -1 | 178.59 | 83.02 | -23.76 |
| 5 | F5 | 0 | 0 | 0 | 191.77 | 80.89 | -35.98 |
| 6 | F6 | -1 | -1 | 0 | 220.31 | 67.9 | -31.39 |
| 7 | F7 | 0 | 1 | -1 | 195.9 | 58.56 | -21.7 |
| 8 | F8 | -1 | 0 | 1 | 209.03 | 78.03 | -48.03 |
| 9 | F9 | 0 | -1 | -1 | 200.7 | 59.02 | -15.7 |
| 10 | F10 | 0 | 0 | 0 | 190.29 | 80.39 | -35.01 |
| 11 | F11 | 1 | 1 | 0 | 171.34 | 72.43 | -32.6 |
| 12 | F12 | 0 | 1 | 1 | 191.98 | 68.02 | -45.9 |
| 13 | F13 | 0 | 0 | 0 | 190.98 | 76.45 | -35.53 |
| 14 | F14 | -1 | 1 | 0 | 202.8 | 65.21 | -34.87 |
| 15 | F15 | 0 | 0 | 0 | 191.99 | 80.01 | -35.87 |
| 16 | F16 | 1 | 0 | 1 | 161.8 | 88.92 | -53.5 |
| 17 | F17 | 0 | -1 | 1 | 195.2 | 70.2 | -45.9 |

**Table 6: ANOVA for Quadratic model for Particle size, Entrapment Efficiency, Zeta Potential**

| Source | PS(Y1) | | | EE%(Y2) | | | ZP(Y3) | | |
|---|---|---|---|---|---|---|---|---|---|
| | F-value | P-value | | F-value | P-value | | F-value | P-value | |
| Model | 118.02 | < 0.0001 | significant | 28.39 | 0.0001 | significant | 152.84 | < 0.0001 | significant |
| A-HS | 960.30 | < 0.0001 | | 43.42 | 0.0003 | | 21.79 | 0.0023 | |
| B-Amount of lipid | 23.52 | 0.0019 | | 3.75 | 0.0942 | | 0.0786 | 0.7873 | |
| C-surfactant conc | 26.96 | 0.0013 | | 28.86 | 0.0010 | | 1292.10 | < 0.0001 | |
| AB | 6.97 | 0.0334 | | 0.6641 | 0.4420 | | 23.45 | 0.0019 | |
| AC | 16.67 | 0.0047 | | 0.0315 | 0.8642 | | 1.11 | 0.3261 | |
| BC | 0.0568 | 0.8185 | | 0.1699 | 0.6925 | | 14.68 | 0.0064 | |
| $A^2$ | 2.55 | 0.1543 | | 16.06 | 0.0051 | | 4.47 | 0.0723 | |
| $B^2$ | 24.87 | 0.0016 | | 155.69 | < 0.0001 | | 17.70 | 0.0040 | |
| $C^2$ | 0.6585 | 0.4438 | | 8.65 | 0.0217 | | 0.8390 | 0.3902 | |
| Lack of fit | 6.56 | 0.0504 | not significant | 1.79 | 0.2881 | not significant | 3.78 | 0.1158 | not significant |

The polynomial eq. 8 suggests that as the A increases Y1 decreases and vice versa, indicative of enhanced particle fragmentation due to increased shear forces. Similarly, an increase in B leads to decrease in Y1 and increase in C increases Y1 attributed to compromised steric stabilization and augmented aggregation tendencies of particles (Agrawal et al., 2021). The p value for A, B and C on Y1 is found to be 0.001, 0.0019, 0.0013 respectively. Similarly, polynomial eq. 9 for Y2 suggests that as the A, B increases and C decreases, the Y2 gets increase effectively. The ANOVA study for the quadratic model for Y2 suggests that A (0.003)and B (0.001) have a significant effect on Y2butC has a less significant effect with ap-value of
0.094.When lipids(B)concentration is high and surfactant (C) concentration is low, the EE% of the particles increases (Y2). This happens because of the change in lipid and surfactant levels that affects EE% (Kim et al., 2019). The polynomial eq. 10 for Y3 suggests that as the A and C significantly affect the value of Y3. The p-value for A and C was found 0.0001and 0.0001, respectively while B has no significant effect as the p-value is found to be 0.7873 which is greater than 0.05. Table 11 depicts the ANOVA for the Quadratic model for PS, EE %, and ZP.

**Polynomial equation**

$$PS = +190.90 - 20.23A + 3.17B - 3.39C + 2.44AB - 3.77AC + 0.22BC - 1.44A^2 = 4.49B^2 + 0.730C^2$$

$$EE = +79.63 + 4.86A - 1.43B + 3.96C - 0.8500AB + 0.1850AC - 0.4300\,BC + 4.07A^2 - 12.69B^2 - 2.99C^2 \quad (9)$$

$$ZP = -35.85 - 1.85A + 0.11B - 14.26C + 2.72AB - 59AC + 2.15BC - 1.16A^2 + 2.30B^2 + 0.50C^2$$

Besides, Design-expert software was used to attain 2D contour plots and 3D surface plots. The surface plots and contour plots for PS, ZP, and EE% is shown in figure 3 and overlay graph are placed in figure 3

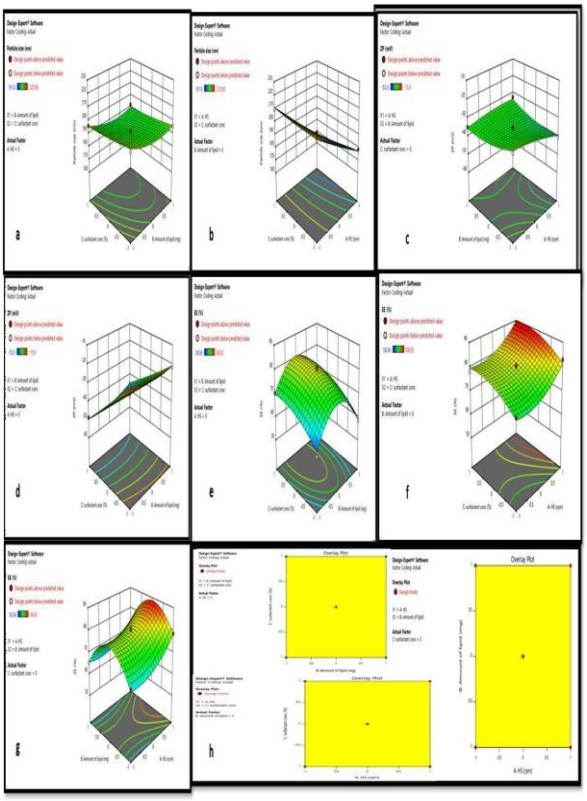

**Figure 3: Surface plot (a) Investigating he Influence of Lipid amount and Surfactant effect**

**on** PS, (b) Exploring the Impact of HS and Surfactant on PS, (c) Exploring the influence of the amount of lipid and HS on ZP, (d) Exploring the influence of the amount of lipid and surfactant on ZP, (e) Exploring the influence of the amount of lipid and surfactant on EE%, (f) Exploring the influence of HS and surfactant on EE%, (g) Exploring the influence of HS and amount of lipid on EE%, (h)Overlay plot for depicting the relation between Surfactant conc. and Amount of lipid, Surfactant conc. and HS, Amount of lipid and HS

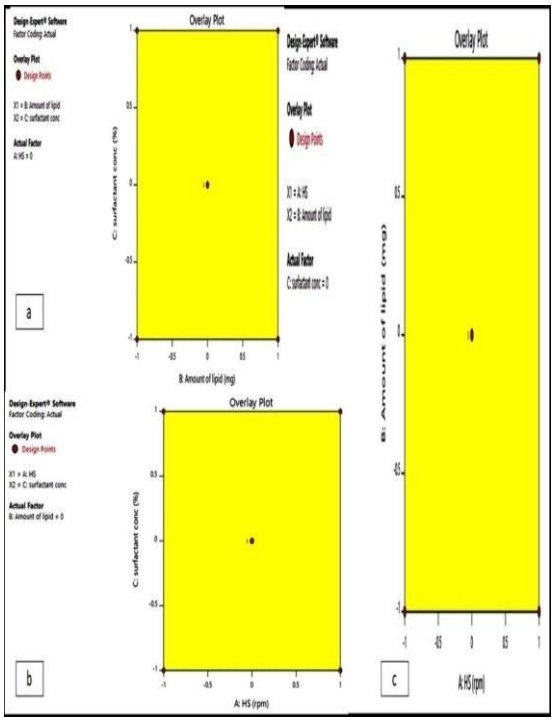


**Figure 4: Overlay plot for depicting the relation between (a) Surfactantconc. and Amount of lipid, (b) Surfactant conc. and HS, (c) Amount of lipid and HS**

Thus, the design of experiment helped in optimization of best possible result for PS, ZP and EE% with different combination of HS, amount of polymer, and surfactant conc. used for the preparation of MPA-NLCs. The best formulation selected based of design of experiment is F-16 among the total 17 batches and used further for the characterization of the MPA-NLC and incorporating into a nanogel form,

**Particle size, poly dispersity index, and zeta potential**

A particle size analyser was used to determine the mean particle size andPDI for MPA-NLCs for 17 batches as depicted in table 9. The mean particle size of the MPA-NLCs varied in a range from 161.80 to 200.31 nm. The particle size for optimized formulation (F-16) was found to be as 161.8 nm. The particle size is an important characteristic of NLCs which governs the bioavailability of the drug at a particular site (Chauhanet al., 2020).It is evident from the previous researches that, the bioavailability improves with decrease in particle size due to increased surface area (Sandrietal.,2014). In the present study, the particle size of was recorded161.8 nm which was in the nanometre range that could easily penetrate through SC and reach the inner layer of the skin. The PDI value was used to evaluate the particle size distribution of NLC in MPA-NLCs. The PDI value for the optimised batch (F- 16), was found to be in a narrow range 0.209. The PDI value demonstrates the distribution of particles of similar size in MPA-NLC. It has been documented that, a PDI value less than 0.5 indicates homogeneous particles in a uniform size range in the formulation (Danaei et al., 2018). The present formulation consists of a PDI value of approximately 0.208 which indicates particles are homogenous and bears good stability with time.

The ZP for batches F1 to F17 was recorded between -15.7 and -53.5 mV and it was found that the optimized batch ZP was noted as to be -53.5 mV. The ZP affects the storage stability of the formulation, reflecting the electrostatic barrier that prevents the aggregation of the particle. The ZP with values between -10 and +10 mV indicates that formulation consist of neutral charges on globules surface whereas, the ZP above +30 mV or below -30 mV indicates high stability of the NLCs globules present in the formulation (Han et al., 2008). A High value for ZP confirms that the oil globules consist of electrostatic repelling interactions, which prevents coalescence among the globule and results in a dispersion that was adequately stable and uniform. In this instance, the NLCs were negatively charged due to the adsorption of hydroxyl ions from water and free fatty acids onto the oil- water interface (Wilson and Green, 2017). If every particle has a strong negative or positive ZP, the tendency for the particles to attract one another gets hindered. However, low ZP levels results in inadequate repulsion to prevent the particles from aggregating and flocculating. The results for PS, PDI, and ZP for different batches fromF-1to F-17arementioned in table 9. Figure 16 a, 16 band 16c depict the value for PS, PDI and ZP of different batches (F-1 to F-17) of MPA-NLC, respectively. Figure 16d and 16 e depicts the average vale for PS and ZP of different batches (F-1 to F-17) of MPA-NLC, respectively.

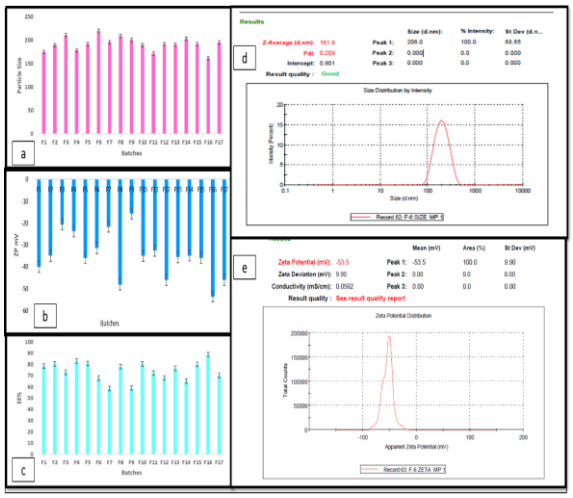

**Figure 5: (a) Particle size of the batch from F1-F16, (b) PDI of batches from F1- F16 and ZP of batches from F1-F16, (d) Average PS of different batches of MPA- NLC. (e) Average ZP**

**Entrapment efficiency and drug loading**

An effective drug delivery system is considered when the significantly high amount of drug is loaded in formulation. In this study, the percentage of non- entrapped drug on the surface of MPA-NLCs was obtained through the centrifugation MPA-NLCs and by analyzing the supernatant in HPLC. Table 9 illustrates the EE% for the MPA-NLCs of the formulation F1-F17, ranging from 88.92% to 59.02%. The optimized batch F16 has an EE % of 88.92% and drug loading capacity of 44.98 ± 2.76%. Based on DoE, it was revealed that a high concentration of lipid and surfactant significantly affect drug entrapment in NLC. The literature tells that a high concentration of liquid lipid remarkably disturbs the arrangement of atoms and molecule which can result in more imperception in the crystal lattice. However, imperfection generates more space which can encapsulate high concentration of drug with better drug EE% (Higel et al., 2016). The results of EE % for F16 batch was at a higher rangeof88.92% due to the presence of oleic acid (30%v/v).The combination of SL and LL results in massive crystal order disturbance, producing enough space for the drug to accommodate. This improves the EE% and DL of the formulation indicating high solubility MPA in 30 % v/v oleic acid. Our findings are in line to the results obtained by Zakie at el., in their study.

**Morphological evaluation Scanning electron microscopy (SEM)**

SEM imaging is an advanced method for understanding size, shape, surface characteristics, and internal structure of the NLCs. It is carried out to understand the physical properties of NLCs, which is used to obtain better results in design and optimization of formulations used for the delivery of drugs in a body. Figure 17 a show the SEM image of the MPA-NLC depicting its spherical shape with a mostly smooth surface and less agglomeration. The lipid purity and concentration helped in maintaining the spherical form of NLC that in turn assist in augmented drug release and the durability of NLC in storage.

**Transmission electron microscopy (TEM)**

TEM, is a robust imaging approach that can be utilized to analyse the internal structure of formulation with high resolution. TEM results demonstrated that the particles present in MPA-NLC formulation were almost spherical and exhibited a uniform size distribution. This indicates that process used to prepare the NLCs was reproducible and yielded uniform particles which was achieved through the homogenization process (figure 17 b).

SEM and TEM images depict the nearly spherical shape of the developed MPA-NLCs. This may be due homogenization process and the use of surfactant. In addition to stabilizing the NLCs, the surfactant lowers surface and interfacial tension (Ortiz et al., 2021). The shape of NLCs, rely on the process that how the lipid layer been modified during the drying process, as rate and extent of evaporation of solvent affects the morphology and structure of the particles. During the drying process, the charges present on the lipid layer changes, that result in change in size and form of the particle (Teer anachaideekul et al., 2007). The deviation from the spherical shape of NLC scan have important implications for their stability and drug delivery properties. For instance, non-spherical particles may have a smaller surface area to volume ratio than spherical ones, which may have an impact on the manner in which they load and release drugs. They may also have different surface properties that can affect their interaction with biological systems.

**Atomic force microscopy (AFM)**

The AFM study helps the researcher in identifying the physical and chemical properties of the particles by evaluating their surface features, particle size, and shape. The surface properties of NLCs, such as their roughness or charge, can have a Significant impact on their stability and interaction with biological systems. Figures 17 c and 17 d show the no-contact mode of the AFM monograph of the optimized (F16) MPA-NLC. The morphological analysis depicts the homogeneity of the samples with low PDI values. The F16 batch represents a mono disperse distribution of NLC with a height of 35.7 nm. Besides spherical-shaped particles were observed with uniform particle sizes. The pores of size 0.01 nm were observed on the

surface that reflects the polymorphic change during drying and creates a 3D representationof the sample. It can be concluded that AFM defines the surface coverage, periodicity, thickness, and width of the NLC.

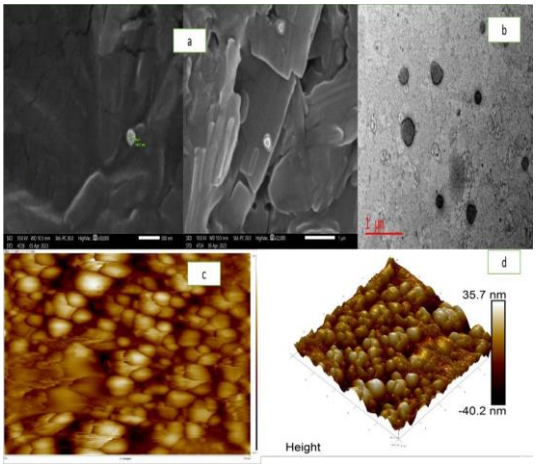


**Figure 6: (a) SEM image for MPA-NLC of the lyophilized powder, (b) TEMimage for MPA-NLC of the lyophilized powder, (c) AFM morphology of an MPA- NLC depicting the roughness, (d) AFM morphology of MPA-NLC depicting the height**

***Fourier transform-infrared spectroscopy***

FTIR (Fourier transform-infrared spectroscopy) was carried out to examine the interaction between the drug and the excipients. The spectra of GB-SL, OA-LL, span 80, MPA, PM, and MPA-NLC were determined through Perkin-Elmer® Pty Ltd./ Spectrum Two FT-IR Spectrometer, Beaconsfield/ UK spectrometer. The spectra were plotted between % transmittance and wavenumber (4000-600 $cm^{-1}$). The MPA's pure spectrum displayed a sharp peak with a C=O stretching band at 1714.39 $cm^{-1}$. Other excipients showed peaks as follows: OA (2922.66 cm-1), GB (2913.05 cm-1), and span 80 (2921.98 $cm^{-1}$). These results have been published in several papers by diverse research organizations (Anand and Srivastava, 2020; J. B. Brubach et al., 2007; RoyChoudhury et al., 2013; Yamawaki and Fujihisa, 2022).

It was observed that the C=0 fatty acid group and CH and $CH_2$stretching aliphatic group was visible in the physical mixture at 1710.94 $cm^{-1}$ and 2921.91 $cm^{-1}$, respectively. This suggests there was no interaction between the drug and the excipients. The characteristic peak at 1647.72 $cm^{-1}$ appeared in the MPA_NLC indicating the peak ofMPA. Moreover, the FTIRgraph (figure 18a) ofF-16 showed amorphous transition and entrapment of MPA in the lipid matrix due to some broad peaks. The FTIR spectra show that the drug and the lipids used to formulate MPA- NLC are compatible in nature.

**X-Ray diffraction(XRD)**

Another useful method for determining the polymorphic structural alterations, phase behaviour, and internal crystalline structure of NLC is X-ray diffraction. It is conducted to analyse the crystallinity or amorphous nature of the drug present as complex as the lipids used (Tetyczka et al., 2019). X-ray analysis revealed that pure MPA was crystalline in nature with diffraction peaks at 5.4, 8.1, 9.9, 10.7, 13.7, and 19.1 in the diffracto gram obtained from the origin pro software. The peaks were intense, sharp, and well-resolved. These results are in agreement with the information provided by Iqbal et al.,(Iqbalet al., 2020). The GB: SL showed major XRD peaks at 5.6, 19.2, 23.1, and 24.2. The data stated by Brubach et al., (Brubach et al., 2007) confirm the peak consistency of GB. The diffractogram of PM exhibited peaksat 5.6,8.3, 9.7, 10.1, 10.9, 19.2, 23.04, and 24.28.The obtained graph suggests that most of the peaks of MPA and SL: GB is visible in the physical mixture. The peaks obtained at 5.6 belongs to both MPA and SL: GB was found to be more intensified. Whereas, other peaks 8.3, 19.2, 23.04, and 24.28 belong to SL: GB, and 9.7, 10.1, and 10.9belong to MPA respectively. Some extra peaks can be seen inthe PM at 13.8 and 22.1 which indicates the presence of some impurities. In the case of MPA-NLC, the XRD peaks were obtained at 5.6, 7.8, 8.3, 11.2, and 15.5. Which indicates that the intensity of peaks for lipids was decreased. This may be due to loss in crystallinity in lipid matrix owing to the interactions between the lipid components of MPA and NLCs. The similar trend of results was obtained by Zarifet al., (Zarif et al., 2012) in their study indicating the loss in crystallinity. Also, the reduced intensity of a peak representing MPA in MPA-NLC indicates the molecular distribution of MPA in the lipid matrix of NLCs.

Here the peaks are present on the diffraction pattern of the formulation which is identical to the drug which confirms the presence of drug on the surface of formulation. Moreover, no distinct MPA crystalline characteristic peak was seen in the MPA-NLC powder. The broad predominated but minor peaks at 2θ scattered angel 19.2° were seen in the MPA- NLC pattern, which may have been caused by the crystalline structure of the SL-GB and cryoprotectants. The findings revealed that MPA in NLC was molecular rather than crystalline. Figure 18 a depicts the XRD graph for MPS-drug, Formulation F- 16, SL-GB, and physical mixture: PM.

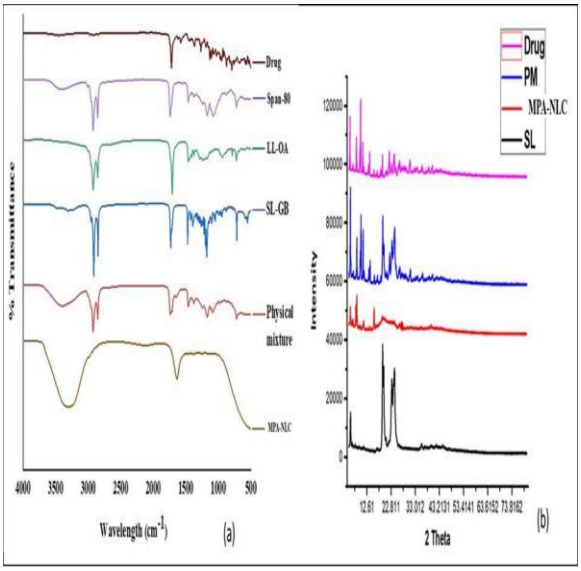


**Figure 7: (a) Drug compatibility study using FTIR for MPA-NLC, MPA, SL-GB, LL-OA, PM, span 80, (b) XRD graph for MPA, MPA-NLC, SL-GB, and physical mixture**

**Differential scanning calorimetry (DSC)**

DSC is frequently used to identify heat gain or loss as a function of temperature resulting from alteration sin a sample's physical or chemical composition. It was employed to examine the drug's crystalline or amorphous form, as well as its presence in the complex. This investigation was done on the basis of variation in temperature and energy at phase transition. Figure 19 shows the DSC curve for MPA, SL-GB, PM and MPA-NLC. The thermogram for MPA showed a melting peak at (191.21°C). The melting peaks for GB-SL was observed at (69.39 °C).These melting peaks were observed in the PM with the same values as in individual graph for MPA and SL-GB. The thermograms of the lyophilized MPA-NLC did not exhibit a melting peak for the MPA at approximately 191.21°C. This indicates that the MPA in the MPA-NLC was not present in a crystalline state, but rather in an amorphous state that formed a solid solution within the nanoparticles' matrix. The lack of the MPA's endothermic peak serves as evidence that it was encapsulated within the NLC in a non-crystalline form.

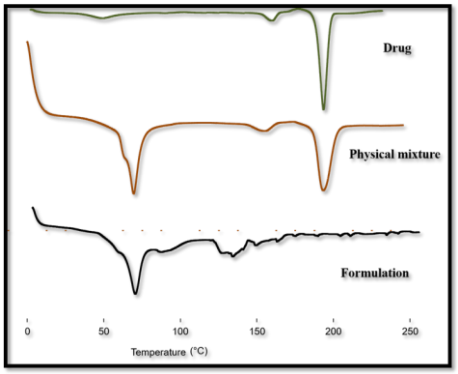


**Figure 8:** Differential scanning calorimetry curves of MPA, physical mixture containing MPA and SL-GB, MPA-NLC

**Stability studies**

The stability studies were carried out to study the effects of temperature and humidity conditions on the formulation's stability overtime. The aim of this study was to analyse the shelf life of the developed formulation and to identify any potential stability issues that may arise during storage or transport. After 1-monthof storage of MPA-NLC at stability condition 4 ± 2°C, was rejected owing to very high particle size (2727 nm). The remaining formulation were continued for 3-month stability studies at 25 ±2°C/65% RH and 40 ±2°C/75% RH condition. After 3-month of stability study, the formulation kept at 40 ±2°C showed high values for in the PS, PDI, and ZP parameters. These changes could indicate a loss of stability and potential degradation of the formulation. The formulation kept at 25 ±2°C/65% RH wascontinuedfora6-month stability study. After 6-month, the formulation at 25 ±2°C/65% RH was found to be unstable due to an enhancement of PS and PDI. It was concluded that the formulation kept at 25 ±2°C showed stability for 3 months with PS (268.1 nm), PDI (0.289), and ZP (-52.8). Table 12 shows the stability data of developed formulation MPA-NLC for 6months.The PS of MPA-NLC was found to be increased at 4 ±2°C and 40 ±2°C, due to Brownian motion, where particles were continuously colliding with each other. This might cause particle aggregation due to Vander Waals's attractive forces generating a much larger floc. As a result, it's crucial to carryout stability studies under different storage conditions in order to determine the factors that can cause particle aggregation and other stability problems. This study helps in designing appropriate storage and handling conditions to ensure the stability and efficacy of the drug .

**Table 7: Stability data of MPA-NLC for 6 months at different stability conditions**

| Condition | Stability at 25±2°C/65% RH | Stability at 4±2°C | Stabilityat40±2°C/ 75 % RH |
|---|---|---|---|
| **1-month study** | | | |
| Particlesize (nm) | 151.8 | 2727 | 365.8 |
| PDI | 0.251 | 0.247 | 0.594 |
| ZetaPotential (mV) | -53.4 | -49.9 | -59 |

| 3-monthstudy | | | |
|---|---|---|---|
| Particlesize (nm) | 268.1nm | 1473nm | 263.7 |
| PDI | 0.289 | 0.139 | 0.322 |
| ZetaPotential (mV) | -52.8 | -54.8 | -29.1 |
| **6-monthstudy** | | | |
| Particlesize (nm) | 754.3nm | 978.3nm | 474nm |
| PDI | 1 | 1 | 0.227 |
| ZetaPotential (mV) | -60 | -55 | -35.5 |

**Preparation of MPA-NLC nanogel**

Since, MPA-NLC has a low viscosity, it must be transformed into a gel to facilitate application and increase skin contact duration. For this purpose, MPA- NLC were entrapped in Carbopol 934 for the formation of MPA-NLC loaded nanogel and characterized for drug content, pH, rheological studies, spreadability, texture analysis, skin permeation study, dermatokinetic study and for analysing the anti-psoriatic potential of MPA nanogel against imiquimod-induced psoriasis in mice.

**Drug content and pH**

The developed MPA-NLCs nanogel's (1 g) showed 96% of drug content for MPA. The value ofdrug content revealed that MPAwas evenlydistributed inMPA- NLC nanogel. The stability of formulation was determined by measuring the pH of the MPA-NLC nanogel (range 6.0 to 6.8). Any change in pH indicates the chemical reaction that has occurred in the final product affecting its quality. Hydrolysis of fatty acid ester generating free fatty acids indicated a decrease in pH of the formulation. Ofnote,inthe current study,the developed formulation, whenstored at 25± 2°C/65 % RH, showed no change in pH up to 90 days.

**Viscosity**

The viscosity of topical preparation is an important parameter that impacts spreadability, contact time, and adhesiveness to the skin. To understand this parameter, a viscosity study was performed for MPA-NLC nanogel, MPA-gel, and blank gel and the findings of the study are shown in the table 13. The MPA-NLC nanogel had 13.03 ps viscositywhereas 7.46 ps and 3.46 ps was observed for MPA- geland blankgelrespectively. It was concluded that MPA-NLC nano gelbearsgood viscosity as compared to MPA-gel and blank gel. Earlier studies in the literature demonstrated that a decrease inshear rate causes an increase in the viscosity of any formulation (Narayana et al., 2009). Presence of Carbopol 934 (1% w/w) in the developed MPA-NLC nanogel helped in attaining good viscosity and pseudoplastic behaviour (shear thinning). Of note, this behaviour is preferred for topicalapplication and helps in attaining ideal spreadability at the site of application.

**Spreadability**

Spreadability is used to assess the effectiveness of the nanogel formulation to spread over the skin, while its application. The more the formulation spreads on to the area of application, the better chances of getting penetrated in to the skin. The spreadability of MPA-NLC nanogel (35.14 g.cm/sec), MPA gel (22.76 g.cm/sec), and blank formulation (8.01 g.cm/sec) were carried out and results of the study revealed that the spreadability of MPA-NLC nanogel was best and thus it could be suitable after topical application. Besides, it advocated that less time couldbe required for the nanogel to get spread over the skin and attaining required permeation of drug across the different layers of skin.

**Texture analysis**

Texture analysis defines the mechanical characterization of MPA-NLC nanogel, MPA-gel, and blank-gel. A graph between force-time is obtained, where the peak height defines the hardness of the gel formation. The hardness for MPA-NLC nanogel, MPA-gel, and the blank gel obtained were 0.4±0.01,0.1±0.02 N, and 0.09±0.02 N respectively. The cohesiveness demonstrates the structural recovery of the gel and found as -256.45 ±0.02 g, -112±0.03 g, and -57.04 ± 0.03 g for MPA-NLC nanogel, MPA gel, and blank-gel respectively. The result of texture analysis, spreadability, and viscosity of the formulation are mentioned in table 13, while figure 20 gives information about the texture analysis and spreadability. Other parameters such as firmness, consistency, and adhesiveness were also analysed and are depicted in table 13. A topical gel formulation should have excellent cohesiveness, high adhesiveness, and low hardness. High adhesiveness provides prolonged retention of gelonthe skin which increases the contact time.Hardness is a measure of resistance to compression, which determines the affluence of gel exclusion from the container. The obtained value for the hardness of MPA-NLC nano gel was found to be greater than MPA-gel indicating a good value for the hardness. The cohesiveness of the obtained formulation was found to be low. Thus, the gel formed bears good hardness and adhesiveness. A change in the parameter of texture analysis was observed, if the pH range changed from 6-10. The pH of the nanogel was maintained by the addition of triethylamine (Hurler et al., 2012).

**Table 8: Texture Analysis, Spreadability, and Viscosity of the MPA-NLC nanogel, MPA-gel and Blank gel**

| Texture Analysis parameter | MPA-NLC nanogel | MPA-gel | Blank-gel |
|---|---|---|---|
| Hardness | 0.4±0.01N | 0.1±0.02N | 0.09±0.02 N. |
| Adhesiveness | -1.13±0.18 N Sec | -4.36±0.22 N sec | -4.48±0.22 N sec |
| Cohesiveness | -256.45±0.02g | -112±0.03g | -57.04±0.03 g |
| Firmness | 433.1g | 231..89g | 84.60g |
| Consistency | 2095.43g/sec | 1234.28g/sec | 724.53g/sec |
| Spreadability | 35.14g.cm/sec | 22.76g.cm/sec | 8.01g.cm/sec |
| Viscosity | 13.03ps | 7.46ps | 3.46ps |
| Shearrate | 8.406gsec | 1.23gsec | 0.087gsec |

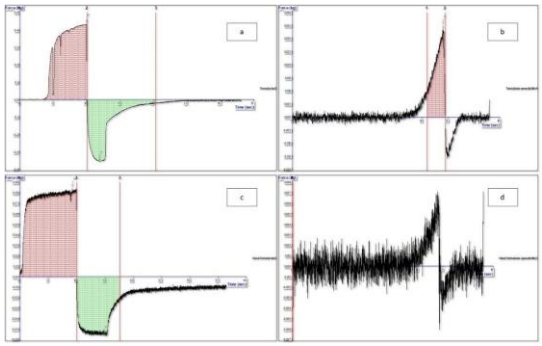

**Figure 9: Texture analysis for (a) MPA-NLC nanogel, and(b), blankgel, Spreadibility study for (c) MPA-NLC nanogel, and (d) blank formulation**

**In-vitro release studies and kinetics**

An in-vitro release studies was conducted to determine the release of MPA from NLCs dispersion using Franz diffusion cells for 48 hrs. The in-vitro release studies were compared between MPA-NLC,MPA-solution, MPA-gel, and MPA NLC nanogel. Figure 21 a show that MPA was successfully released from MPA- NLC. The data is represented as standard deviation of n=3 replicates. At first burst release of drug was observed trailed by sustained release. The sustained release significantly maintains the constant drug levels at the target site. The percentage of MPA release up to 4 hrs was found to be 48.55%.The burst release could be helpful in increased penetration of the drug. It was observed that MPA-NLC showed 67.87 % of drug release up to 48 hrs in comparison to MPA-solution showing 18.19 % of release. MPA-NLC formulation showed 48.55 % of drug release in 4 hrs followed by sustained release of about 20.63 %. The slower release was attained due to the presence of GB-SL containing hydrophobic long-chain fatty acids esters that was containing the lipophilic drug. Also, the MPA release pattern was significantly impacted by the span 80 employed in the formulation that played significant role in reducing the interfacial tension that in tun augmented the release of drug from the formulation. Similarly, MPA-NLC nano gelshowed43.61% of drug release upto 48 hrs in comparison to MPA gel showing 26.47 % of drug release. Initially burst release was seen as a result of some amount drug that was not entirely encapsulated in the gel matrix. The remaining amount entrapped inside the NLC coreprovided the sustained release later. These results are in line to the observations attained by the Iriventi & Gupta.

By fitting the release data into different models, including first order, zero order, Higuchi, Hixson Crowell, and Korsmeyer Peppas equations, the release kinetic of developed formulation was determined. A graph was plotted according to model applied and r2was determined.

The most significant R2 value was considered based on excellent fit. The data obtained from the equation is depicted in figure 21b, 21c, 21d, 21e and in the table 14. According to the obtained findings, it can be concluded that the in-vitro drug release of MPA in PBS (pH 6.8) followed Higuchi models demonstrating that the diffusion mechanism was mostly responsible for the drug release.

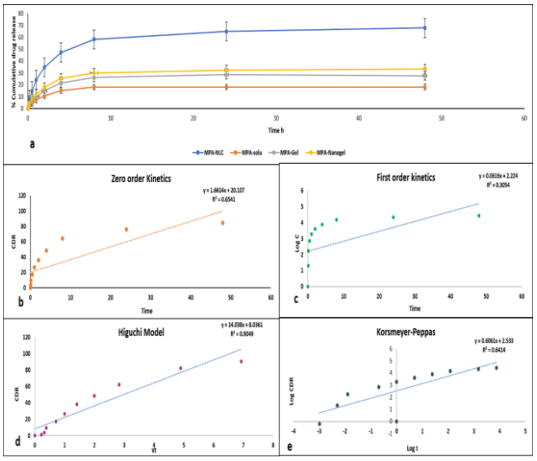


**Figure 10: (a) Comparative In-vitro drug release profile of MPA from MPA-NLC, MPA-solution, MPA-Gel, MPA-NLC nanogel. The data are shown as standard deviation of n = 3 replicates. Kinetic model of release from MPA-NLC at 6.8 phosphate buffer (b). Zero-order kinetics, (c). First Order kinetics, (d). Higuchi model, (e) Korsmeyer Peppas Model.**

**Table 9: Release kinetics of MPA-NLC using different models**

| Models | $R^2$ | | | |
|---|---|---|---|---|
| | MPA-NLC | MPA-solution | MPA-Gel | MPA-NLC nanogel |
| Zero-Order Kinetics | 0.6541 | 0.6875 | 0.6908 | 0.6396 |
| First Order Kinetics | 0.3054 | 0.3478 | 0.3299 | 0.3339 |
| Higuchi Model | 0.9049 | 0.9008 | 0.9031 | 0.8699 |
| Korsmeyer Peppas Model | 0.641 | 0.8028 | 0.8397 | 0.6862 |

## CONCLUSION

The present study focuses on the development, optimization and characterization of MPA-NLC and its therapeutic evaluation in imiquimod-induced model of psoriasis in albino mice. MPA loaded NLCs (MPA-NLCs) have been prepared using psoriasis in hot melt technique followed by homogenization and sonication. The different excipient used for the preparation of MPA-NLC were glyceryl behenate, oleic acid, and span 80. Pareto and Box Behnken designs were used in the experiment's strategy to optimize MPA-NLCs and determine how the amount of lipid, homogenization speed, and surfactant concentration affect particle size, zeta potential, and entrapment effectiveness. A total 17 batch (F1-F17) were determined by the design of experiment and on the basis of PS, ZP and EE% batch F16 was selected as optimised batch and used for further studies. It was found that MPA-NLC exhibit nano-range particle size, narrow PDI, negative ZP, high EE% and drug loading. The morphological determination of MPA-NLC was carried out to determine the physical characteristic of MPA-NLC using SEM, TEM and AFM. It was found that MPA-NLC were spherical in shape with smooth surface, less agglomeration and uniform size distribution. Further, FTIR, XRD and DSC studies were also performed to determine the compatibility and structural change in MPA- NLC. The FTIR study showed amorphous transition and entrapment of MPA in the lipid matrix due to the presence of broad peaks in the spectra.

The FTIR spectra shows that the drug and lipids used to formulate MPA-NLC are compatible in nature. The XRD studies revealed that MPA present in NLC was molecular rather than crystalline in nature. The MPA's endothermic peak obtained in DSC study serves as evidence that it was encapsulated within the NLC in a non-crystallineform. The formulation exhibited remarkable physical stability over 90 days of storage at 25 ±2°C/65% RH. The MPA-NLCs was found to have low viscosity, therefore, it must be transformed into a gel to facilitate application and increase skin contact duration on skin. The MPA-NLC nanogel showed good viscosity and pseudoplastic behaviour with good spread over the skin to attained required permeation of drug across the different layers of skin.

The texture analysis showed a good hardness and adhesiveness, and low cohesiveness. The in-vitro release study suggests that formulation showed sustained release of MPA following Higuchi models which demonstrates the diffusion mechanism. The results for skin permeation study showed that the alteration in the skin due to inflammation and keratinocytes hyperproliferation helps in greater penetration of drug through the skin and has the capability to reach the specific cells or tissues in the skin with higher retention. Further, the results of dermatokinetic study suggests that the MPA-NLC nanogel formulation has a favourable pharmacokinetic profile and ability to attain augmented permeation of drug across the skin-layers compared to MPA-gel. It is imperative to analyse the toxicity profile of MPA-NLC nanogel to determine its compatibility for topical application. The study revealed that MPA-NLC nanogel was safe up to the doses of 50, 1000 or 2000mg/kg, when applied on the dorsal skin region of mice. Further, anti-psoriatic efficacy of developed MPA-NLC nanogel's was examined in the imiquimod induced psoriasis mice model. It is noteworthy that administration MPA-NLC nanogel at 5 mg/kg and 10 mg/kg significantly reduced the psoriatic score and inflammatory markers in mice, similar to standard(clobetasol propionate). Besides, the MPA-NLC nanogels substantially depressed the serum's levels of TNF- and IL-6, indicating that the newly developed formulation has a strong anti-inflammatory activity. Additionally, the effect of MPA-NLC nanogel was also evaluated on oxidative stress markers. The mice treated with MPA-NLC nanogel exhibited enhanced levels of protective enzymes and reduced levels of oxidative stress markers. Therefore, MPA-NLC nanogel possessed promising antioxidant properties, thus resulting in reduced oxidative damage and free radical stress. Moreover, MPA-NLC nanogel ameliorated abnormal skin physiology by reducing epidermal hyperplasia, vesicular formation, and keratosis, thus exerting protective effects, and exhibiting promising anti-psoriatic potential in mice. Overall, these findings indicates that the developed MPA-NLC nanogel for topical administration could be a rational strategyto attain augmented therapeutic attributes of MPA, without or having limited serious adverse effects in psoratic individuals. However, further studies are required to validate the efficacy of developed MPA- NLC nanogel in clinical subjects bearing psoriasis and

related issues.

**REFERENCE**


1. Richa; Roy Choudhury, A., Synthesis of a novel gellan-pullulan nanogel and its application in adsorption of cationic dye from aqueous medium. Carbohydr Polym 2020, 227, 115-291.
2. Adi, A. C.; Christanto, C.; Rachmawati, H.; Adlia, A., vitamin e-based folic acid nanoemulsion: formulation and physical evaluation for oral administration. pharm nanotechnol 2019, 7 (4), 304-313
3. Sinha, P.; Srivastava, S.; Mishra, N.; Singh, D. K.; Luqman, S.; Chanda, D.; Yadav, N. P., Development, optimization, and characterization of a novel tea tree oil nanogel using response surface methodology. Drug Dev Ind Pharm 2016, 42 (9), 1434-45
4. Tchewonpi Sagu, S.; Huschek, G.; Bonick, J.; Homann, T.; Rawel, H. M., A New Approach of Extraction of alpha-Amylase/trypsin Inhibitors from Wheat (Triticum aestivum L.), Based on Optimization Using Plackett-Burman and Box-Behnken Designs. 2019, 24
5. Bonomo, L.; Abittan, B. J.; Hashim, P. W.; Karki, C.; Mason, M.; Lebwohl, M., Combination Use of Systemic Therapies in Psoriasis: Baseline Characteristics from the Corrona Psoriasis Registry. J Drugs Dermatol 2019,731-740.
6. Sonzogni, A. S.; Yealland, G.; Kar, M.; Wedepohl, S.; Gugliotta, L. M.; Gonzalez, V. D. G.; Hedtrich, S., effect of delivery platforms structure on the epidermal antigen transport for topical vaccination. 2018, 102-125.
7. Panonnummal, R.; Jayakumar, R.; Sabitha, M., Comparative anti-psoriatic efficacy studies of clobetasol loaded chitin nanogel and marketed cream. Eur J Pharm Sci 2017, 96, 193-206
8. Sanzhakov, M. A.; et al,. The in vivo study of the medicinal composition property of doxorubicin as a part of colloidal nanoparticles with the address fragment]. Biomed Khim 2016, 62 (2), 150-3.
9. Divya, G.; Panonnummal, R.; Gupta, S.; Jayakumar, R.; Sabitha, M., Acitretin and aloe-emodin loaded chitin nanogel for the treatment of psoriasis. Eur J Pharm Biopharm 2016, 107, 97-109.
10. Porwal, P. K.; Upmanyu, N., Assessment by HPLC of the degradation behavior of acitretin under hydrolytic, oxidative, photolytic and thermal stress conditions. Acta Pharm Sin B 2014, 4 (6), 438-46.
11. Rote, A. R.; Kumbhoje, P. A.; Bhambar, R. S., UV-visible spectrophotometric simultaneous estimation of paracetamol and nabumetone by AUC method in combined tablet dosage form. Pharm Methods 2012, 3 (1), 40-3.
12. Mousaviasl, S.; Saleh, T.; Shojaosadati, S. A.; Boddohi, S., Synthesis and characterization of schizophyllan nanogels via inverse emulsion using biobased materials. Int J Biol Macromol 2018, 120 (Pt A), 468-474.
13. Shen Q, Liu R, Tan S, Xu X, Fang J, Li R. Advances in pathogenesis and nanoparticles (NPs)-mediated treatment of psoriasis. Front Immunol. 2022;13:108.
14. Kokol P, Blažun Vošner H, Završnik J. Application of bibliometrics in medicine: a historical bibliometrics analysis. Health Info Libr J. 2021;38(2):125–138.
15. Ninkov A, Frank JR, Maggio LA. Bibliometrics: methods for studying academic publishing. Perspect Med Educ. 2022;11(3):173–176.
16. Synnestvedt MB, Chen C, Holmes JH. CiteSpace II: visualization and knowledge discovery in bibliographic databases. AMIA Annu Symp Proc. 2005;2005:724–728.
17. Hirsch JE. Does the H index have predictive power? Proc Natl Acad Sci U S A. 2007;104(49):19193–19198.
18. Zhang X, Zhou Y, Wei N, et al. A bibliometric analysis of heart failure with preserved ejection fraction from 2000 to 2021. Curr Probl Cardiol. 2022;47(9):101243.
19. Fang JY, Lee WR, Shen SC, Fang YP, Hu CH. Enhancement of topical 5-aminolaevulinic acid delivery by erbium:YAG laser and microdermabrasion: a comparison with iontophoresis and electroporation. Br J Dermatol. 2004;151(1):132–140.
20. Chen R, Zhai YY, Sun L, et al. Alantolactone-loaded chitosan/hyaluronic acid nanoparticles suppress psoriasis by deactivating STAT3 pathway and restricting immune cell recruitment. Asian J Pharm Sci. 2022;17(2):268–283.
21. Rapalli VK, Waghule T, Gorantla S, Dubey SK, Saha RN, Singhvi G. Psoriasis: pathological mechanisms, current pharmacological therapies, and emerging drug delivery systems. Drug Discov Today. 2020;25(12):2212–2226.
22. Santos AC, Rodrigues D, Sequeira JAD, et al. Nanotechnological breakthroughs in the development of topical phytocompounds-based formulations. Int J Pharm. 2019;572:118787.
23. Paiva-Santos AC, Silva AL, Guerra C, et al. Ethosomes as nanocarriers for the development of skin delivery formulations. Pharm Res. 2021;38(6):947–970.
24. Zhang Y, Gong S, Liu L, et al. Cyclodextrin-coordinated liposome-in-gel for transcutaneous quercetin delivery for psoriasis treatment. ACS Appl Mater Interfaces. 2023;15(34):40228–40240.
25. Saka R, Jain H, Kommineni N, Naveen C, Khan W. Enhanced penetration and improved

therapeutic efficacy of bexarotene via topical liposomal gel in imiquimod induced psoriatic plaque model in BALB/c mice. J Drug Delivery Sci Technol. 2020;58:101691.
26. Wadhwa S, Singh B, Sharma G, Raza K, Katare OP. Liposomal fusidic acid as a potential delivery system: a new paradigm in the treatment of chronic plaque psoriasis. Drug Deliv. 2016;23(4):1204–1213.
27. Knudsen N, Rønholt S, Salte RD, et al. Calcipotriol delivery into the skin with PEGylated liposomes. Eur J Pharm Biopharm. 2012;81(3):532–539.
28. Jain H, Geetanjali D, Dalvi H, Bhat A, Godugu C, Srivastava S. Liposome mediated topical delivery of Ibrutinib and Curcumin as a synergistic approach to combat imiquimod induced psoriasis. J Drug Delivery Sci Technol. 2022;68:103103.
29. Wang W, Shu GF, Lu KJ, et al. Flexible liposomal gel dual-loaded with all-trans retinoic acid and betamethasone for enhanced therapeutic efficiency of psoriasis. J Nanobiotechnology. 2020;18(1):80.
30. Dadwal N, Amisha, Singh D, Singh A. Quality-by-Design approach for investigating the efficacy of tacrolimus and hyaluronic acid-loaded ethosomal gel in dermal management of psoriasis: in vitro, ex vivo, and in vivo evaluation. AAPS Pharm Sci Tech. 2023;24(8):220.
31. i Y, Xu F, Li X, et al. Development of curcumin-loaded composite phospholipid ethosomes for enhanced skin permeability and vesicle stability. Int J Pharm. 2021;592:119936.
32. Costanzo M, Esposito E, Sguizzato M, et al. Formulative study and intracellular fate evaluation of ethosomes and transethosomes for vitamin D3 delivery. Int J Mol Sci. 2021;22(10).
33. Pandey SS, Shah KM, Maulvi FA, et al. Topical delivery of cyclosporine loaded tailored niosomal nanocarriers for improved skin penetration and deposition in psoriasis: optimization, ex vivo and animal studies. J Drug Delivery Sci Technol. 2021;63:102441.
34. Shah P, Goodyear B, Dholaria N, Puri V, Michniak-Kohn B. Nanostructured non-ionic surfactant carrier-based gel for topical delivery of desoximetasone. Int J Mol Sci. 2021;22(4).
35. Yang X, Tang Y, Wang M, et al. Co-delivery of methotrexate and nicotinamide by cerosomes for topical psoriasis treatment with enhanced efficacy. Int J Pharm. 2021;605:120826.
36. Mittal S, Ali J, Baboota S. Enhanced anti-psoriatic activity of tacrolimus loaded nanoemulsion gel via omega 3 - Fatty acid (EPA and DHA) rich oils-fish oil and linseed oil. J Drug Delivery Sci Technol. 2021;63:102458.
37. Wan T, Pan J, Long Y, et al. Dual roles of TPGS based microemulsion for tacrolimus: enhancing the percutaneous delivery and anti-psoriatic efficacy. Int J Pharm. 2017;528(1–2):511–523.
38. Sahu S, Katiyar SS, Kushwah V, Jain S. Active natural oil-based nanoemulsion containing tacrolimus for synergistic antipsoriatic efficacy. Nanomedicine (Lond). 2018;13(16):1985–1998.
39. Algahtani MS, Ahmad MZ, Ahmad J. Nanoemulsion loaded polymeric hydrogel for topical delivery of curcumin in psoriasis. J Drug Delivery Sci Technol. 2020;59:101847.
40. Benigni M, Pescina S, Grimaudo MA, Padula C, Santi P, Nicoli S. Development of microemulsions of suitable viscosity for cyclosporine skin delivery. Int J Pharm. 2018;545(1–2):197–205.
41. Pandey SS, Maulvi FA, Patel PS, et al. Cyclosporine laden tailored microemulsion-gel depot for effective treatment of psoriasis: in vitro and in vivo studies. Colloids Surf B Biointerfaces. 2020;186:110681.